Arabian Journal of Chemistry (2021) 14, 103314

King Saud University

Arabian Journal of Chemistry

www.ksu.edu.sa
www.sciencedirect.com

ORIGINAL ARTICLE

Adsorption performance and mechanism of mycotoxin on montmorillonite modified by organosilicon grafting

Mengxia Lv [a], Jiaqi Mao [b], Ying Zhou [c], Renxian Zhou [b], Jianmin Zhou [a],*

[a] School of Pharmaceutical Sciences, Wenzhou Medical University, Wenzhou, Zhejiang 325035, PR China
[b] Institute of Catalysis, Zhejiang University, Hangzhou 310028, PR China
[c] Zhejiang Ecological and Environmental Monitoring Center, Hangzhou 310012, PR China

Received 17 May 2021; accepted 3 July 2021
Available online 14 July 2021

KEYWORDS

Deoxynivalenol;
Mycotoxin;
Modified-montmorillonite;
Acid treatment;
Organosilicon

Abstract A series of modified montmorillonites were prepared by acid modification method prior to the organosilicon grafting. Aflatoxin B_1, zearalenone and deoxynivalenol (DON) were selected to evaluated the mycotoxin adsorption performance of modified montmorrillonites. The experimental results suggest that under acidic conditions, the higher the charge density in the covalent orbital of the active group, the stronger the interaction between it and the DON molecule, and the better the corresponding modified montmorillonite adsorbs DON. Silicified montmorillonite with active groups of cyano group and methacryloyloxy group has the best adsorption performance for DON, and the adsorption degree are 51.6% and 39.0%, respectively. However, under alkaline terms, due to the hydrolysis of active groups, the adsorption degree of montmorillonite on DON dropped steeply.

1. Introduction

Mycotoxins are toxic secondary metabolites produced by mold in the growth process of substrate (feed, food, and raw materials) (Wang et al., 2018; Phillips et al., 2008). They are a kind of low molecular weight compounds with diverse structure. Among the means of detoxification, physical adsorption has attracted wide attention due to its low cost, good safety and addability to animal feed and food. Montmorillonite with layered structure is a kind of mycotoxin adsorbents which has been reported and commercialized (Farooq et al., 2020). However, practical applications of natural montmorillonite is limited by its layered microstructure and the active adsorption sites are covered by impurity minerals and not exposed, resulting in a low utilization rate (Nguyen Van et al., 2020; Pavlidou and Papaspyrides, 2008). In addition, the unmodified montmorillonite has strong hydrophilicity, so it only has a strong adsorption effect on aflatoxin B_1(AFB_1), which is a typical kind of polar mycotoxin. But natural montmorillonite has basically invalid on adsorption for non-polar and weak polar

---

* Corresponding author.
E-mail address: zhoujm93@163.com (J. Zhou).

Peer review under responsibility of King Saud University.

Production and hosting by Elsevier

https://doi.org/10.1016/j.arabjc.2021.103314

mycotoxins, such as zearalenone (ZEA) and deoxynivalenol (DON). Therefore, the development of high-efficiency and broad-spectrum montmorillonite adsorbents is the key to the removal of more mycotoxins.

After acid treatment, the montmorillonite was deeply peeled, and the ordered layers of montmorillonite were broken in different degrees, which exposing more active sites for adsorption of non-polar or weak polar organosilicon (Mao et al., 2020; Gozali Balkanloo et al., 2020). In addition, surfactant intercalation is another common type of modification method which favors montmorillonite to bind low-polar and hydrophobic mycotoxins by introducing surfactants into the interlamellar space (Zhang, 1993).

However, both methods mentioned above cannot effectively improve the adsorption degree of montmorillonite for DON due to its poor molecular planarity and large steric hindrance. Therefore, seeking a method to modify the edges or external surface of the montmorillonite sheet may become a new idea to improve its adsorption efficiency for DON (Mao et al., 2020).

Organosilicon modification is a technology that has attracted much attention in the field of modification of montmorillonite in recent years (Mosaleheh and Sarvi, 2020; Choi and Shin, 2020). In the process of organosilicon alkylation, the exposed silicon hydroxyl (Si-OH) and aluminum hydroxyl (Al-OH) on the edges, external surface and interlayer space of the montmorillonite can be reacted with silane coupling agents with hydrolytic groups (such as methoxy and halogen elements) to form new Si-O covalent bonds. In addition, in the process of organosilanization, some groups with special reactivity (such as amino, cyano and ester groups, etc.) will be introduced into the surface of the montmorillonite sheet, which can effectively improve the selective adsorption capacity of montmorillonite for mycotoxin with various molecular structure (Choi and Shin, 2020).

In this paper, five kinds of organosilicon molecule with different structures were grafted onto the surface of acid-treated modified montmorillonite. On this basis, the organosilicon/cetylpyridinium chloride (CPC) composite modification was further prepared. By evaluating the adsorption performance of various modified montmorillonites for AFB_1, ZEA and DON, and combining XRD, elemental analysis, N_2 adsorption and desorption and DR-FTIR and other analytical testing techniques, this paper studies the effect of the crystal structure, specific surface area and silane active group of modified montmorillonite on its adsorption efficiency of mycotoxin.

2. Materials and methods

2.1. *Materials*

The montmorillonite-rich clay powder (assigned as MMT) was natural mineral from China. It is composed of above 73.6% Ca^{2+}-montmorillonite, 22.1% microcline and 4.2% quartz, based on X-ray powder diffraction analysis. The surfactant CPC and organosilanes supplied by sinopharm chemical reagent Co. Ltd were used for the preparation of modified montmorillonites. The mycotoxins such as AFB_1, DON and ZEA, were purchased from J&K Chemical Co. Primary stock solutions of each mycotoxin (100 µg/mL) were prepared in chromatographic grade methanol and stored at 2 °C. The formulas of organosilanes and names of samples are given as follows:

Fomula	Structural Formula	Organosilicon grafted samples	Organosilicon/CPC modified samples
$C_9H_{23}NO_3Si$	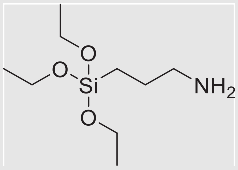	AMMT-NH2-1	/
$C_8H_{22}N_2O_3Si$	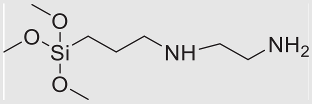	AMMT-NH2-2	/
$C_4H_{10}ClSi$	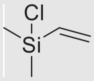	AMMT-C2H4	AMMT-CPC-C2H4
$C_9H_{19}NO_3Si$	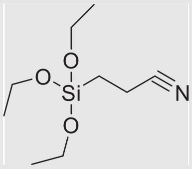	AMMT-CN	AMMT-CPC-CN
$C_{10}H_{20}O_5Si$	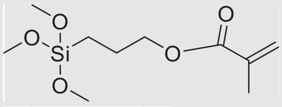	AMMT-CO2	AMMT-CPC-CO2
$C_{12}H_{10}Cl_2Si$	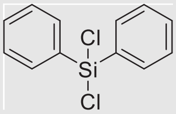	/	AMMT-CPC-C6H6

2.2. Preparation of modified montmorillonite

2.2.1. Preparation of acid-modified montmorillonite

A certain concentration of 100 mL sulfuric acid solution was poured into a three necked flask, 5 g natural montmorillonite MMT was added under magnetic stirring, and then heated to 150 °C for condensation reflux reaction for 3 h. After the reaction, it was cooled to room temperature and centrifuged, and the solid product was washed repeatedly with deionized water to remove unreacted sulfuric acid until no sulfate ion was detected. Dry in an oven at 60 °C for 12 h and grind to powder to prepare a series of acid-modified montmorillonites, labeled AMMT-3 where y represents the acid/clay (w/w) ratio of 0.3 was calculated using the dry weight of clay and 98% H_2SO_4.

2.2.2. Preparation of organosilicon modified montmorillonite

Preparation of organosilicon grafted modified montmorillonite: 2 g of dry AMMT-3 powder was mixed with 60 mL of acetone solvent under N_2 protection to isolate the air. The suspension was stirred at room temperature for 30 min. and then quickly added 1 g of organosilicon. The reaction was proceeded at 80 °C and continue to condense and reflux under N_2 protection for 6 h. After the reaction, it was cooled to room temperature, centrifuged, and washed with acetone several times to remove excess organosilicon. It was dried in an oven at 60 °C for 12 h to obtain organosilicon modified montmorillonite.

Preparation of organosilicon/CPC compound modified montmorillonite: 2 g organosilicon modified montmorillonite was dispersed in 50 mL distilled water for 30 min. and then added 1 g CPC. The suspension was stirred over night at room temperature. All the products were washed free of halogen anions Cl^- followed by drying at 60 °C.

2.3. Evaluation of mycotoxin adsorption performance

2.3.1. Standard curve

High performance liquid chromatography-mass spectrometry (HPLC-MS) to draw the corresponding curve of deoxynivalenol(DON) concentration: use external standard method for calibration. The specific steps are: prepare a series of DON mixed solutions with different concentrations (100, 50, 25, 5 and 2 ng/mL), measure the response values with HPLC-MS, and draw a standard curve of instrument reading-DON concentration.

2.3.2. Mycotoxin adsorption test method

8.0 g NaCl, 0.1 g $MgCl_2{\cdot}6H_2O$, 0.2 g KCl, 0.13 g $CaCl_2{\cdot}2H_2O$ and 0.2 g KH_2PO_4 were dissolved in HPLC-grade purified water to prepare 1 L phosphate buffer solution (PBS). The PBS solution was divided into two equal parts, and the pH was adjusted to 2.8 and 8.0 with H_3PO_4 and Na_2HPO_4 to simulate the acid-base environment in the animal's stomach and intestine.0.5 mL, 100 μg / ml AFB_1, ZEA and DON solutions were added into two 250 mL volumetric flasks respectively. PBS solution with pH value of 2.8 and 8.0 was used to fix the volume, and the mixed solution with the concentration of three mycotoxins of 200 ng / ml was prepared. Use a pipette gun to transfer each 5 mL of the mold mixture was transferred to a test tube containing 20 mg of montmorillonite to be tested (montmorillonite: mycotoxin = 20,000:1), then place it in a shaker at 37 °C for 4 h and then centrifuge. Transfer 4 mL of supernatant to a centrifuge tube. The unadsorbed mycotoxins in the supernatant were extracted with 4 mL of methyl *tert*-butyl ether, the extraction was repeated 3 times, and the upper organosilicon phase after separation was transferred to another centrifuge tube. At a temperature of 40 °C in a water bath, use N_2 to purge the organosilicon solvent in the centrifuge tube until all of it evaporates. Then measure 200 μL of acetonitrile (HPLC grade), add it to the centrifuge tube after the N_2 purge, and fully shake on the in-situ shaker for 1 min to completely dissolve the mycotoxins attached to the tube wall, and detect by HPLC-MS.

In order to avoid the error caused by the calculation of the adsorption degree when the extraction rate of MTBE for mycotoxins is less than 1, two groups of mycotoxins with pH of 2.8 and 8.0 were used as the blank experimental group, and the concentrations of three mycotoxins were detected under the same experimental conditions.

$$\textit{Adsorption degree} = (1 - X_1/X_0) * 100\% \ (X = a, b, c)$$

where, a_1(ng/mL), b_1(ng/mL) and c_1(ng/mL) are the concentrations of unadsorbed AFB_1, ZEA and DON; a_0(ng/mL), b_0(ng/mL) and c_0(ng/mL) are the concentrations of the three mycotoxins under the conditions.

2.3.3. Mycotoxin testing equipment and testing conditions

In this test, HPLC-MS analysis technology is used to detect the concentration of mycotoxins. The single injection volume is 5 μL. The instrument specifications and detection conditions used are as follows.

Agilent 1290 Infinity High Performance Liquid Chromatograph: 1290 Infinity II diode array detector (HDR-DAD), high pressure infusion pump (Agilent 1290). Chromatographic column: Zorbax SB C-18 column (2.1 mm × 150 mm; 3.5 μm), mobile phase A is deionized water, mobile phase B is acetonitrile, the gradient elution program is shown in Table 1 and the set flow rate is 0.3 mL/min.

Agilent 6460 mass spectrometer: drying gas flow rate 5 L/min, drying gas temperature 325 °C, atomizing gas pressure 45psi, vaporization temperature 350 °C. Positive ion mass spectrometry (ESI + /MS) conditions: capillary voltage 3 KV, cone voltage 0 V. Negative ion mass spectrometry (ESI-/MS) conditions: capillary voltage 3.5 KV, cone voltage 500 V.

2.4. Characterization method of montmorillonite

2.4.1. X-ray diffraction (XRD)

Advance 8diffractometer type X-ray powder diffractometer (Bruker Corporation, Germany) was used to determine the

Table 1 Gradient elution procedures of HPLC.

Elution time/min	Mobile phase A[%]	Mobile phase B[%]
0.00	90	10
5.00	15	85
8.00	5	95
10.00	5	95
10.50	65	35
13.50	65	35

phase composition of montmorillonite. The test conditions are: Cu Kα rays (λ = 0.154 nm), tube voltage is 40 KV, tube current is 40 Ma, scanning range is 2–40° (2θ), scanning rate is 5°/min, step size is 0.02°.

2.4.2. *Specific surface area and pore structure*

The specific surface area (BET calculation model), pore volume and pore size (BJH calculation model) of montmorillonite were measured using the TrisStarII automatic surface and porosity analyzer (Micromeritics, America) at liquid nitrogen temperature (−196 °C). Before testing, each sample must be vacuum pretreated at 120 °C for 6 h.

2.4.3. *Elemental analysis*

The Vario MICRO cube type element analyzer (Elementar, Germany) was used to determine the C and N element content in organosilicon grafted modified montmorillonite or organosilicon/CPC compound modified montmorillonite. The pressures of high-purity oxygen and high-purity helium are 0.20–0.22 MPa and 0.15–0.16 MPa, respectively. Quartz combustion tube temperature is 950–962 °C; O_2 flow rate is 30 mL/min, burning for 50 s.

2.4.4. *Diffuse reflectance infrared spectroscopy (DRFTIR)*

Nicolet 6700 Fourier Transform Infrared Spectroscopy (ThermoFisher Scientific, America) was used to characterize the molecular structure of modified montmorillonite. Weigh 100 mg of montmorillonite and place it in the sample chamber. First, at 60 °C, use Ar pretreatment with a flow rate of 90 mL/min to purge for 30 min, and then start to collect infrared spectrum data. The scanning range is 4000–1000 cm^{-1}, and the spectral resolution is It is 4 cm^{-1}. After deducting the Ar background from the collected raw data, the infrared spectrum of the sample is obtained.

2.4.5. *Water absorption tests*

Water absorption tests were carried out in a small chamber containing a saturated aqueous solution of potassium nitrate which fixes the relative humidity within 94.62 ± 0.66% (D'Amico et al., 2014). Before tests, all the samples were dried under vacuum at 120 °C for 6 h and then were enclosed in chamber until constant mass. The water absorption Ma(%) was calculated as:

$$M_e * (\%) = (-1) \times 100\%$$

where M_0 and M_e are the mass of samples before and after moisture adsorption.

3. Results and discussion

3.1. *XRD results*

Fig. 1**a and b** are the XRD spectra of organosilicon modified and organosilicon/CPC composite modified montmorillonite respectively. Table 2 shows the peak positions and crystal plane spacing faces of each sample {001} spacing. The interlayer spacing of the two aminosilane grafted montmorillonites AMMT-NH2-1 and AMMT-NH2-2 increase obviously (Fig. 1**a**). Although the molecular chain of organosilicon grafted by the former is shorter than that of the latter, its d_{001} value is larger. In response to this abnormal experimental result, Filomena carried out molecular dynamics simulation calculations on the process and the arrangement of aminosilane grafted on the surface and came to the following conclusions: Firstly, molecules silanes with longer chains and multiple amino functional groups tend to form more intermolecular or intramolecular hydrogen bonds; secondly, the longer silane molecular chain and the more number of nonpolar group methylene groups leading to the stronger the hydrophobicity. Therefore, based on the above two reasons, silane with long molecular chain and large number of amino groups strongly interact between the montmorillonite layers, resulting in smaller spacing between the montmorillonite layers. For the other three organosilicon grafted modified montmorillonites AMMT-C2H4, AMMT-CN and AMMT-CO2, the {001} crystal plane spacing did not change significantly compared with AMMT-3.

From the following elemental analysis and infrared spectroscopy, it can be seen that the above three kinds of organosilicon have been successfully grafted on the surface of montmorillonite. Therefore, it can be inferred that the reason for the small change in the layer spacing is as follows: (1) The grafting amount of organosilicon molecules is higher on the outer surface and edge of the sheet layer, but less on the inner surface between the layers; (2) Compared with aminosilane, the above three organosilicon active groups cannot form hydrogen bonds with water, and the water

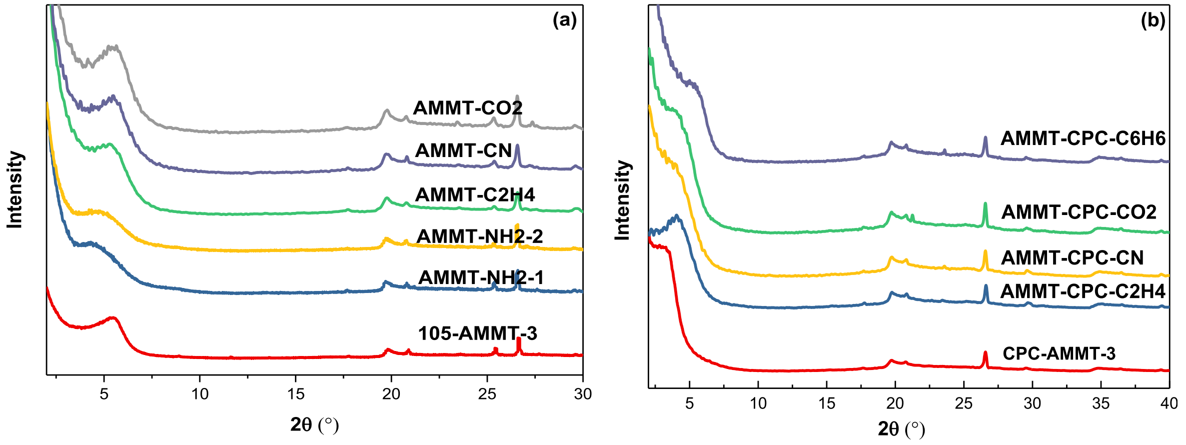

Fig. 1 XRD profiles of organosilicon (a) and organosilicon/CPC complex (b) modified montmorillonites.

Table 2 XRD data of organosilicon and organosilicon/CPC complex modified montmorillonites.

Samples	2θ (°)	d_{001} (Å)	Samples	2θ (°)	d_{001} (Å)
AMMT-3	5.5	15.9	CPC-AMMT-3	3.4	25.8
AMMT-NH2-1	4.4	19.9	CPC-C2H4	4.0	21.9
AMMT-NH2-2	4.6	19.1	CPC-CN	4.3	20.3
AMMT-C2H4	5.5	16.2	CPC-CO2	4.2	20.9
AMMT-CN	5.5	15.9	CPC-C6H6	5.5	16.0
AMMT-CO2	5.5	15.9			

Table 3 Elemental analysis data of organosilicon and organosilicon/CPC complex modified montmorillonites.

Samples	C (%)	N (%)	Grafted amount of organosilane[a] (mmol/g)	Intercalated amount of CPC [b] (mmol/g)
AMMT-3	/	/	/	/
AMMT-NH2-1	5.83	1.69	1.62	/
AMMT-NH2-2	8.28	2.84	1.38	/
AMMT-C2H4	1.58	0.00	0.33	/
AMMT-CN	3.67	1.17	1.02	/
AMMT-CO2	4.98	0.03	0.69	/
CPC-AMMT-3	23.55	1.28	/	0.91
CPC-C2H4	16.25	0.80	0.39	0.57
CPC-CN	16.67	1.77	0.70	0.56
CPC-CO2	17.65	0.70	0.70	0.50
CPC-C6H6	16.34	0.69	0.42	0.49

[a] Calculated by C%.
[b] Calculated by N%.

between the layers is easy to lose, leading to the crystal plane spacing decreases.

From Fig. 1**b** and Table 2, we can see that the peak position of the {001} crystal plane of CPC-AMMT-3 is 3.4°, and the interlayer spacing is 25.8 Å, which is significantly higher than that of the organosilicon/CPC composite modified montmorillonite. It shows that the organosilicon grafted on the inner surface of the interlayer will affect the arrangement of surfactant molecules between the layers, making the angle between the CPC molecules and the lamellae smaller, which leads to the reduction of the {001} crystal plane spacing.

3.2. Elemental analysis results

Through the C and N element analysis techniques, the grafting amount of different types of organosilicon and CPC molecule intercalation in the modified montmorillonite can be

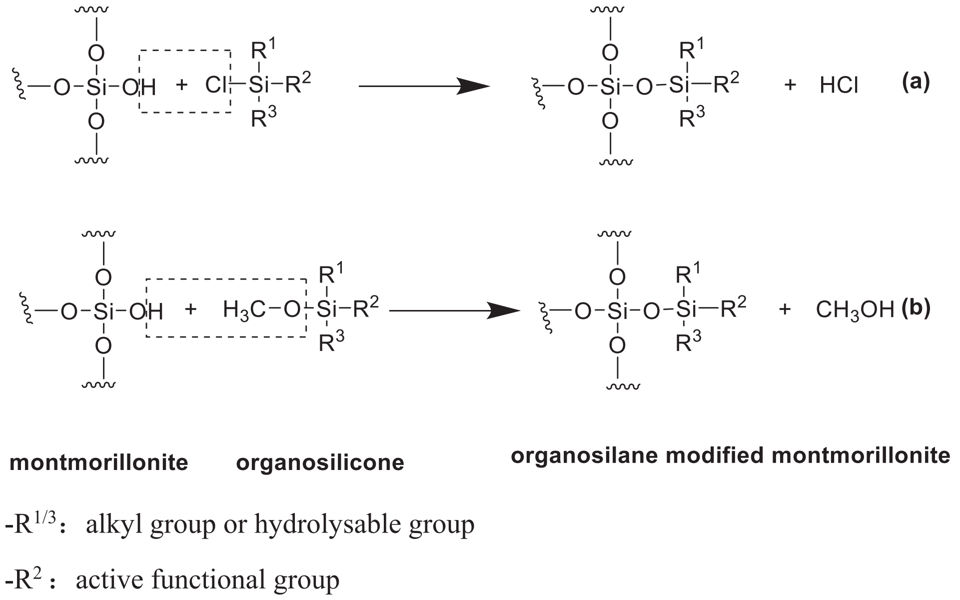

Fig. 2 Reaction scheme for the montmorillonite surface modification with chlorosilanes (a) and methoxylsilane (b).

calculated. As shown in Table 3**.** Among the five organosilicon-modified montmorillonites, AMMT-C2H4 has the smallest organosilicon grafting amount (0.33 mmol/g), which is significantly smaller than that of the other four samples. Observing the molecular structures of different silanes, we can see that the hydrolyzed group of vinyl silane and montmorillonite is the halogen element -Cl, while the hydrolyzed group of other silanes is methoxy —OCH$_3$. Figs. 2**a and** 4**b** respectively show the reaction mechanism of organosilane with SCl and —OCH$_3$ as hydrolysis groups and montmorillonite. From this, it can be inferred that the influence factors of silane molecular structure on the reaction conversion rate are as follows:(1) The stronger the polarity of the hydrolysis group, the more easily the bond from the silane molecule to be broken; (2) The smaller the polarity of the active group -R^2, the more electrons in the molecule are concentrated on the side of the hydrolysis group, which is also beneficial to hydrolysis of covalent bond between the group and the silicon atom. Therefore, the organosilicon with hydrolysis group —OCH$_3$ is easier to react with montmorillonite than that with hydrolysis group —Cl, resulting to the larger grafting amount.

On the other hand, among the four silanes whose hydrolyzed groups are methoxy groups, in descending order of grafting amount: AMMT-NH2-1 (1.62) > AMMT-NH2-2 (1.38) > AMMT-CN (1.02) > AMMT-CO2 (0.69). This sequence is opposite to the order of the polarity of the active group, which proves that the above conjecture (2) is correct: The greater the polarity of the active group -R^2, the less conducive to the silanization reaction of montmorillonite, and the lower the grafting amount of silane.

The intercalation amount of CPC molecules in CPC-AMMT-3 reached 0.91 mmol/g. Compared with CPC-AMMT-3, the intercalation amount of CPC in the other four organosilicon/CPC composite modified montmorillonites was significantly reduced. According to the previous research results of this subject, the reaction of surfactant molecules with montmorillonite mainly consists of two stages: Firstly, a large number of surfactant molecules enter the interlayer after exchange with interlayer cations; when the interlayer ion exchange reaches saturation, its molecular chains will be adsorbed to montmorillonite in a form of non-ion exchange (ion dipole force, van der Waals force) on sheet surface. Therefore, it can be inferred that for the organosilicon/CPC composite modified montmorillonite, the organosilicon molecules grafted on the inner surface and end surface of the montmorillonite layer will prevent the surfactant molecules from entering

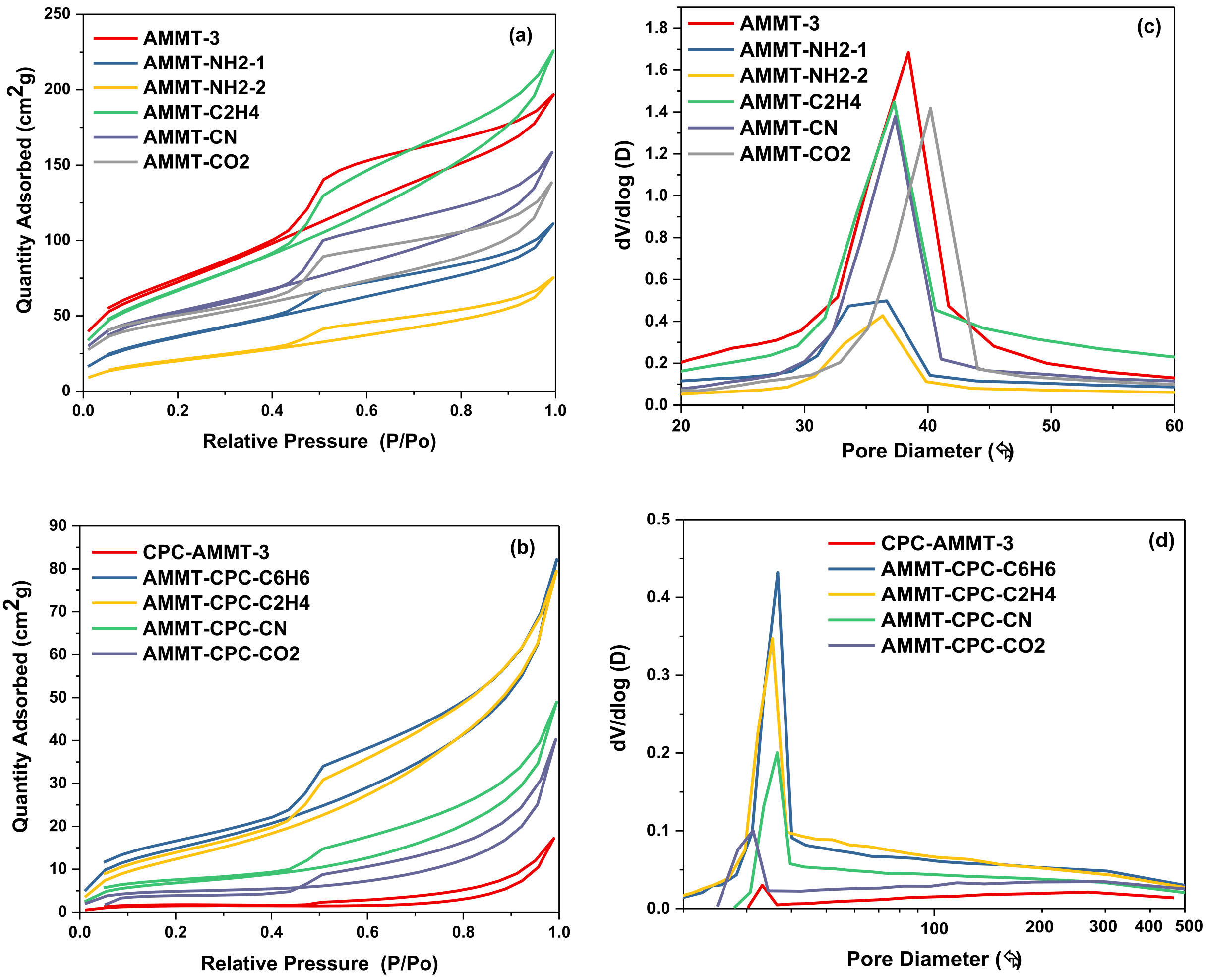

Fig. 3 N$_2$ adsorption-desorption isotherms (a,b) and pore size distribution (c,d) of organosilicon and organosilicon/CPC complex modified montmorillonites.

Table 4 Textural properties of organosilicon modified montmorillonite and organosilicon/CPC complex modified montmorillonite.

Samples	S_{BET} (m^2/g)	V (cm^3/g)	Pore size (Å)	Samples	S_{BET} (m^2/g)	V (cm^3/g)	Pore size (Å)
AMMT-3	267	0.30	45.6	CPC-AMMT-3	4.8	0.03	222
AMMT-NH2-1	136	0.17	50.6	CPC-C_2H_4	50	0.12	98.6
AMMT-NH2-2	76	0.12	60.8	CPC-CN	24	0.08	124
AMMT-C2H4	249	0.35	56.2	CPC-CO_2	16	0.06	157
AMMT-CN	187	0.25	52.4	CPC-C_6H_6	54	0.13	90.1
AMMT-CO2	164	0.21	52.3				

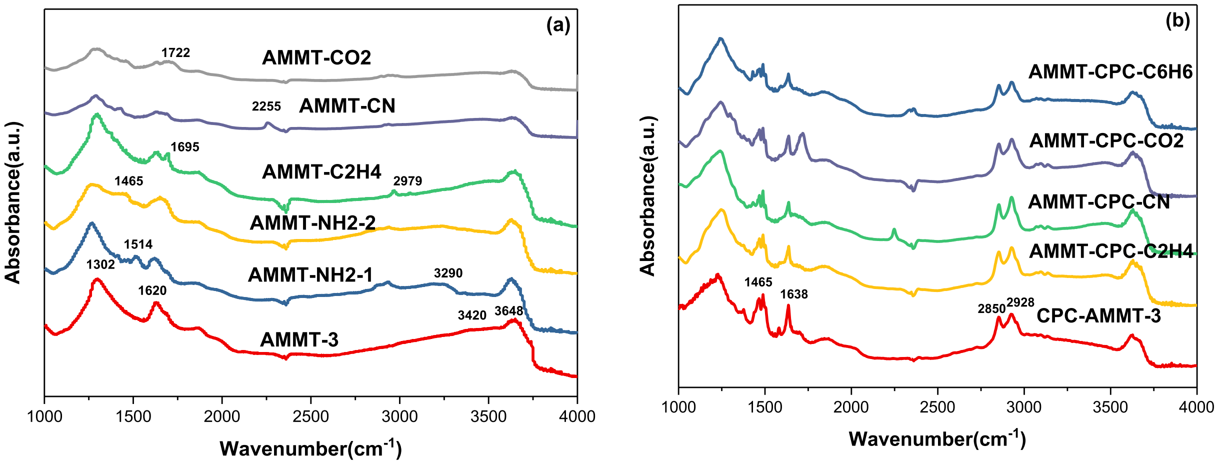

Fig. 4 DRFTIR spectra of organosilicon (a) and organosilicon/CPC complex (b) modified montmorillonites.

the interlayer by ion exchange with hydrogen ions. Organosilicon molecules grafted on the outer surface of montmorillonite will also greatly reduce the adsorption amount of surfactant molecules on the surface of the sheet, ultimately leading to a significant reduction in the amount of CPC intercalation.

3.3. Specific surface area and pore structure results

The N_2 adsorption and desorption isotherms and pore size distribution curves of organosilicon modified or organosilicon/CPC composite modified montmorillonite are shown in Fig. 3**.** It can be seen from Fig. 3**a and b** that the N_2 adsorption and desorption isotherms and hysteresis loop types of all organosilicon-modified or organosilicon/CPC composite modified montmorillonites are respectively type IV And H4 type, which are both consistent with AMMT-3. It means that montmorillonite still has a mesoporous structure after organosilicon silicon modification or organosilicon silicon/CPC composite modification.

It can be seen from Table 4 that the specific surface area and pore volume of the five organosilicon-modified montmorillonite clays are in order from large to small: AMMT-C2H4 > AMMT-CN > AMMT-CO2 > AMMT-NH2-1 > AMMT-NH2-2. Among them, the grafted organosilicon molecular chain in AMMT-NH2-2 is the longest. And hydrogen bonds are formed between molecules to interact, so the blockage of the mesopores of montmorillonite is the most serious, resulting in the smallest specific surface area and pore volume. It can be seen from Fig. 3**c** that the pore size distribution of the five organosilicon-modified montmorillonites is concentrated in the range of 30–40 Å. However, the average pore diameter of each sample in Table 4 is greater than 50 Å, which indicates that the organosilicon molecules are unevenly distributed on the surface of montmorillonite. The interlaced layers will form a small number of large pores, which increases the average pore diameter of montmorillonite.

It can be seen from Fig. 3**c** and Table 4 that compared with the texture data of CPC-modified montmorillonite CPC-AMMT-3, the specific surface area and pore volume of the organosilicon silicon/CPC composite modified montmorillonite are significantly increased large, and its average pore size is smaller than CPC-AMMT-3. According to the results of elemental analysis discussed above, the organosilicon molecules grafted on the surface and edge of montmorillonite hinder CPC molecules from entering the interlayer. Therefore, compared with CPC-AMMT-3, the organosilicon/CPC composite modified montmorillonite has CPC alkyl molecular chain does not block the pores of montmorillonite seriously, and its specific surface area and pore volume are also large.

3.4. DRFTIR

Fig. 4**a** and **b** are the diffuse reflectance infrared spectra of organosilicon modified or organosilicon/CPC composite modified montmorillonite in the wavenumber range of 4000–1000 cm^{-1}. It can be seen from Fig. 4**a** that the strong absorption peak at 1302 cm^{-1} in the infrared spectrum of AMMT-3 is attributed to the stretching vibration of montmorillonite Si-O, including two forms of in-plane and out-of-plane vibration; The absorption peak at 1620 cm^{-1} is attributed to the —OH bending vibration peak of the interlayer water of montmorillonite, while the stretching vibration peak appears at 3420 cm^{-1}. The absorption peak at 3648 cm^{-1} is produced by the —OH stretching vibration connected to aluminum in the octahedron. By comparing AMMT-3 and various organically modified montmorillonites, it can be seen that the —OH peaks intensity of the modified montmorillonite at 1620 cm^{-1} and 3420 cm^{-1} weaken in different degrees, which means that the interlayer water of the organically modified montmorillonite is greatly reduced and the hydrophobicity is enhanced.

In addition, the infrared spectra of organosilicon-modified montmorillonites all show the corresponding characteristic absorption peaks of the active groups. The absorption peak of AMMT-NH2-2 and AMMT-NH2-1 montmorillonite grafted with aminosilane in the range of 1300–1550 cm^{-1} is attributed to the stretching vibration of C—N. And the broad peak overlapping with the water —OH peak at 3500–3300 cm^{-1} is the stretching vibration peak of —NH_2. The C═C and ═CH stretching vibration peaks of AMMT-C2H4 appear at 1695 cm^{-1} and 2979 cm^{-1} respectively. The —C≡N stretching vibration peak of AMMT-CN is located at 2255 cm^{-1}; while the absorption peaks of —C═O and C═C groups in AMMT-CO2 appear in the range of 1690–1730 cm^{-1} and overlap each other.

It can be seen from Fig. 4**b** that the absorption peak of CPC-AMMT-3 at 1465 cm^{-1} is attributed to the bending vibration of —CH_2— in the alkyl chain, and its symmetrical and asymmetrical stretching vibration peaks are located at 2850 cm^{-1} and 2928 cm^{-1}, respectively. The peak at 1638 cm^{-1} is formed by the C═C and C═N stretching vibrations on the pyridine ring. For organosilicon/CPC composite modified montmorillonite, the corresponding characteristic absorption peaks of organosilicon and CPC appear in their infrared spectra. For example, CPC-C6H6 has multiple overlapping absorption peaks in 1650–1430 cm^{-1}, which are caused by aromatic C═C stretching vibration. These results also further show that various organosilicons can be successfully grafted on the surface of montmorillonite through substitution reactions, and the montmorillonite modified by organosilicon can also be further inserted with CPC between layers to form the organosilicon/CPC composite modification montmorillonite.

3.5. Adsorption properties of modified montmorillonite to mycotoxins

Figs. 5**a and** 6**a** show the adsorption degree of AFB_1 on organosilicon grafted modified or organosilicon/CPC composite modified montmorillonite. It can be seen from Fig. 5**a** that the adsorption degree of AMMT-3 for AFB_1 reaches 100% under acidic or alkaline conditions. After being modified by different organosilicon, its adsorption degree for AFB_1 is affected at different level. Under acidic conditions, the adsorption degree of AMMT-C2H4, AMMT-CN and AMMT-CO2 to AFB_1 still maintained 100%, but the adsorption degree of these organosilicon grafting modifications to AFB_1 decreased slightly in an alkaline environment. Among these organosilicon grafted modified montmorillonites, the adsorption degree of AMMT-NH2-2 on AFB_1 decreased greatly compared with AMMT-3, which was 93.2% and 89.3% under acidic or alkaline conditions, respectively.

The β-dicarbonyl system of AFB_1 has been found to chelate metal ions within the interlayers or edges to form configuration of hexatomic rings (Kosicki et al., 2016). Otherwise, the two carbon atoms contained in β-dicarbonyl group are partial positively charged and could easily be attracted by negatively charged montmorillonite surface. According to our previous research, the layers of raw montmorillonite were exfoliated after acid treatment, exposing more active sites at terminal and external surface for adsorption of AFB1 (Wang et al., 2019).

In this paper, organosilicon molecular chain grafted in AMMT-NH2-2 is long and has two amino groups, which easily form hydrogen bonds and cross-link with each other. As a result, the adsorption sites of the montmorillonite surface and the end face of AFB_1 are covered, resulting in a decline in its adsorption performance.

It can be seen from Fig. 6**a** that the adsorption degree of CPC-AMMT-3 on AFB_1 under acidic or alkaline conditions is 96.7% and 96.8%, respectively. Compared with AMMT-3, its adsorption degree on AFB_1 is also slightly reduce. The adsorption degree of AFB_1 by organosilicon/CPC composite modified montmorillonite is close to that of CPC-AMMT-3. The adsorption performance of CPC-CN on AFB_1 under acid or alkaline conditions is slightly improved, and the adsorption degree are both over 97%. However, compared with montmorillonite modified by organosilicon grafting, the adsorption degree of AFB_1 on these four organosilicon/CPC composite modified montmorillonites under acidic conditions is slightly lower. According to the above elemental analysis results, the intercalation amount of CPC molecules in the organosilicon/CPC composite modified montmorillonite is significantly lower than that of CPC-AMMT-3. This indicates that the affinity between the molecular chains of organosilicon grafted on the surface of montmorillonite and AFB_1 is weaker than the affinity between CPC and AFB_1, and the presence of molecular chains between layers of organosilicon will weaken the intermolecular force of between CPC and mycotoxins to some extent.

Increasing the interlayer spacing of montmorillonite or the introduction of weakly polar molecules to enhance the hydrophobicity of the lamellae can both increase its adsorption degree of ZEA (Figs. 5**b and** 6**b**). Compared with AMMT-3, the adsorption degree of CPC-AMMT-3 on ZEA is significantly improved. But for montmorillonite grafted by organosilicon, since the organosilicon molecules are distributed on the outer surface and edge of the sheet, ZEA can interact with it and be adsorbed without entering the interlayer. Thus, the hydrophobicity will directly affect its the adsorption degree of ZEA, such as AMMT-NH2-1 and AMMT-NH2-2, has the largest interlayer spacing among the five organosilicon modified montmorillonites, but the adsorption degree of ZEA is lower than that of AMMT-C2H4 and AMMT-CO2.

Hydrophilic character of the montmorillonite after the modification treatments could be evaluated by water absorption tests (Wang et al., 2019). As shown in Table 5, it can be seen that the equilibrium water uptake percentage of organosilicon modified montmorillonite from small to large are: AMMT-CO2 (10.2%) < AMMT-NH2-2 (16.1%) < AM

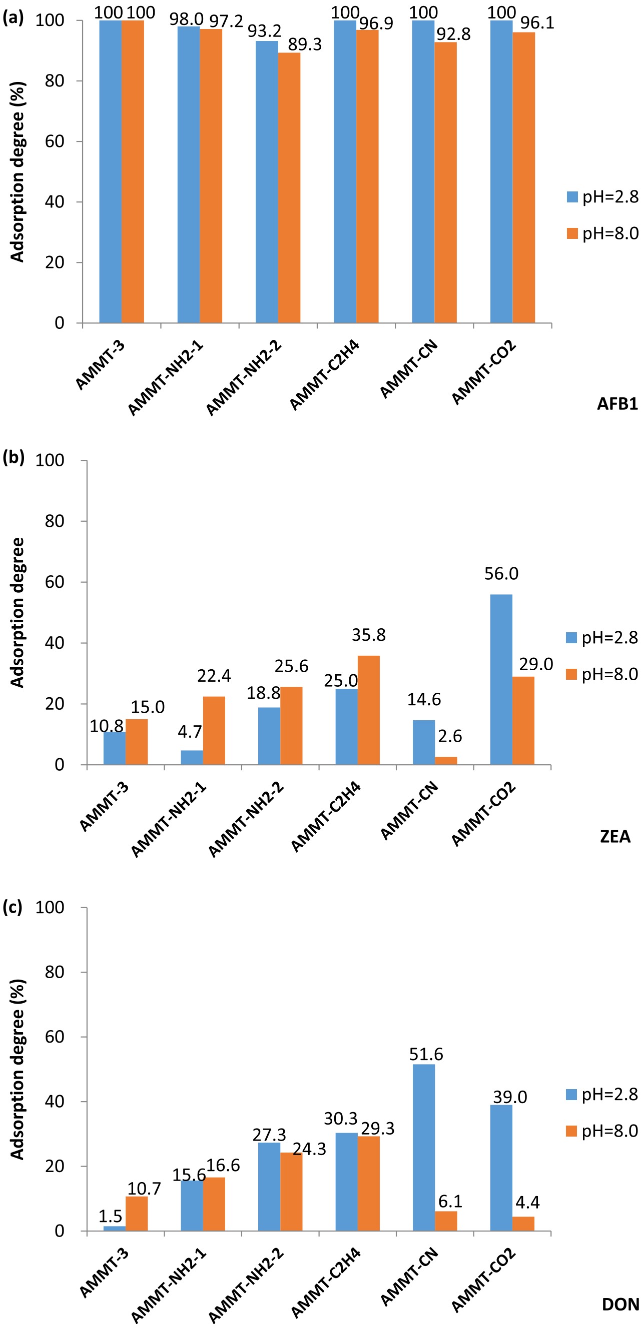

Fig. 5 Adsorption degree of AFB$_1$ (a), ZEA (b) and DON (c) on organosilicon modified montmorillonites. AFB$_1$: Aflatoxin B$_1$, ZEA: zearalenone, DON: deoxynivalenol.

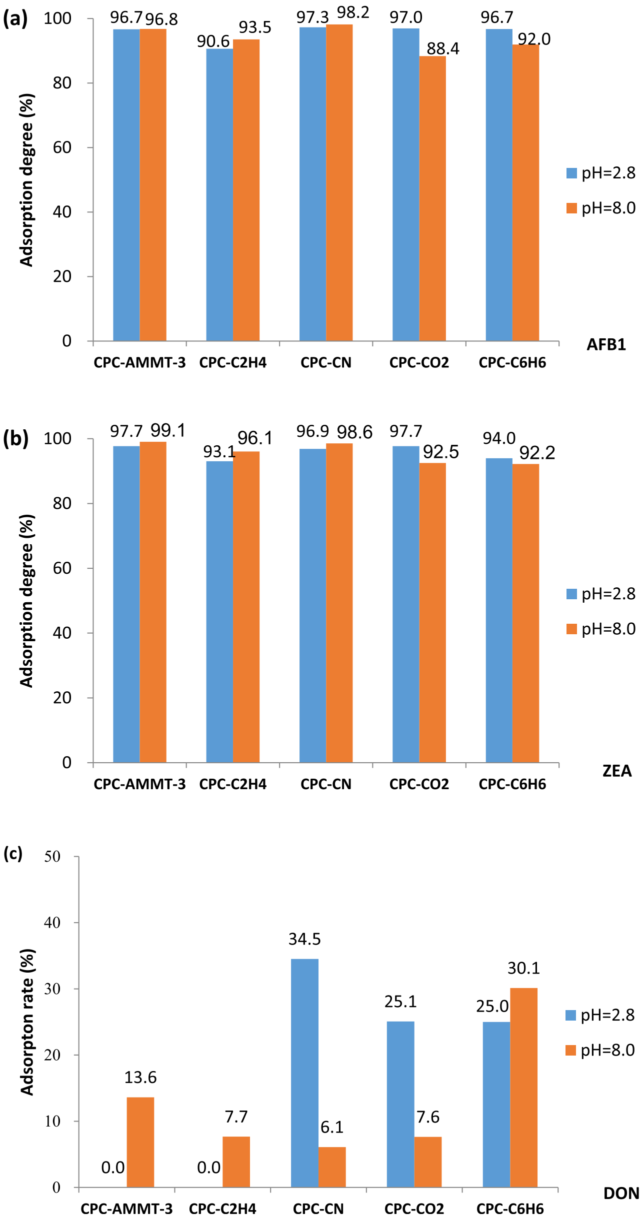

Fig. 6 Adsorption degree of AFB$_1$ (a), ZEA (b) and DON (c) on organosilicon/CPC complex modified montmorillonite.

Table 5 Equilibrium water uptake percentage of organosilicon and organosilicon/CPC complex modified montmorillonites.

Samples	M$_e$*(%)	Samples	M$_e$*(%)
AMMT-3	28.0	CPC-AMMT-3	9.01
AMMT-NH2-1	21.2	CPC-C2H4	14.7
AMMT-NH2-2	16.1	CPC-CN	11.6
AMMT-C2H4	17.7	CPC-CO2	8.10
AMMT-CN	29.0	CPC-C6H6	9.40
AMMT-CO2	10.2		

MT-C2H4 (17.7%) < AMMT-NH2-1(21.2%) < AMMT-CN (29.0%), which shows that AMMT-CO2 has the strongest hydrophobicity, and the order of the hydrophobicity is basically consistent with the results of ZEA adsorption degree. The hydrophobicity of AMMT-C2H4 is slightly weaker than AMMT-NH2-2, which is related to the small amount of organosilicon grafted in AMMT-C2H4 (Table 3), but its adsorption degree of ZEA is still higher than AMMT-NH2-2. For the organosilicon/CPC composite modified montmorillonite, its water absorption and weight gain rate did not change significantly compared with CPC-AMMT-3, and its adsorption degree of ZEA remained above 92%.

The adsorption degree of the DON on the montmorillonite modified by organosilicon is significantly higher than that of

AMMT-3(Figs. 5**c and** 6**c**). For the montmorillonite grafted by organosilicon, under acidic conditions, the adsorption degree of AMMT-CN to DON reached 51.6%, which was significantly higher than AMMT-3 (1.5%). The order of adsorption degree of DON for each sample is: AMMT-CN (51.6%) > AMMT-CO2 (39.0%) > AMMT-C2H4(30.3%) > AMMT-NH2-2(27.3%) > AMMT-NH2-1(16%) > AMMT-3(10.8%). Under alkaline conditions, the adsorption degree of AMMT-C2H4, AMMT-NH2-2 and AMMT-NH2-1 on DON is also significantly improved, especially AMMT-C2H4 reaches 29.3%, which is significantly higher than AMMT-3 (10.8%). However, the adsorption degree of AMMT-CN and AMMT-CO2 on DON dropped sharply to 6.1% and 4.4%, respectively. For montmorillonite modified by organosilicon/CPC compound, no matter under acidic or alkaline conditions, CPC-C6H6 showed good adsorption performance for DON, reaching 25.0% and 30.1%, respectively. However, the adsorption performance of other composite modified montmorillonite for DON has not been improved.

It can be inferred that under acidic conditions, the higher the charge density in the covalent orbital of the active group, the stronger the force between the covalent orbital and the DON molecule, and the better the corresponding modified montmorillonite will adsorb DON. Unfortunately, under alkaline conditions, the adsorption degree of AMMT-CN, AMMT-CO2, CPC-CN and CPC-CO2 on DON drops sharply to below 10%, which may be related to the hydrolysis of two active groups in alkaline environment, It shows that the DON adsorbed in the stomach of the animal may be desorbed in the intestine during the actual application. Therefore, further search for organosilicon modifiers with high charge density and stable chemical properties will become a new direction for improving the DON adsorption performance of montmorillonite in the future.

4. Conclusion

Organosilicon grafted montmorillonite and organosilicon/CPC composite modified montmorillonite were prepared from acid treated montmorillonite AMMT-3 and organic intercalated montmorillonite CPC-AMMT-3, respectively. The effects of different organosilicon grafted montmorillonite on the adsorption of AFB_1, ZEA and DON were investigated. The physicochemical properties of the modified montmorillonite were studied by XRD, elemental analysis, N_2 adsorption and desorption, DRFTIR and water vapor adsorption equilibrium. The conclusions are as follows:

1. In the process of organosilanization, some special reactive groups ((such as amino, cyano, ester, etc.) will be introduced into the surface of the montmorillonite sheet, and the greater the polarity of the organosilicon molecule, the greater the reaction conversion rate. And the adsorption degree of ZEA is improved as the hydrophobicity of montmorillonite modified by organosilicon enhancing. However, the adsorption site of AFB_1 on the surface and edge of the montmorillonite is covered, resulting in a decrease in the adsorption performance of $AFB_{1.}$
2. In the organosilicon/CPC composite modified montmorillonite, the organosilicon grafted on the inner surface of the lamella will affect the arrangement of CPC molecules between the layers and the amount of intercalation. The affinity between CPC and AFB_1 is weaker than that of CPC-AMMT-3, thus reducing its adsorption efficiency for AFB_1. However, the water absorption and weight gain rate of composite modified montmorillonite has no obvious change compared with CPC-AMMT-3, so its adsorption degree of ZEA is maintained above 92%.
3. Under acidic conditions, the higher the charge density in the covalent orbital of the active group, the stronger the force between the covalent orbital of the active group and the DON molecule, and the better the DON adsorption performance of the corresponding modified montmorillonite. Organosilicon grafted montmorillonite with active groups of cyano group and methacryloxy group has the best adsorption performance for DON. However, under alkaline conditions, due to the hydrolysis of active groups, the adsorption degree of montmorillonite to DON dropped sharply to below 10%.

Declaration of Competing Interest

The authors declare that they have no known competing financial interests or personal relationships that could have appeared to influence the work reported in this paper.

Acknowledgments

This project is an experimental and exploratory research. On this basis, we will apply for the National Natural Science Foundation of China. This research did not receive any specific grant from funding agencies in the public, commercial, or not-for-profit sectors. Mengxia Lv and Jiaqi Mao contributed equally to this work.

References

Choi, J., Shin, W.S., 2020. Minerals 10.

D'Amico, D.A., Ollier, R.P., Alvarez, V.A., Schroeder, W.F., Cyras, V.P., 2014. Appl. Clay Sci. 99, 254–260.

Farooq, M., Saeed, M.A., Imran, M., Uddin, G.M., Asim, M., Bilal, H., Younas, M.R., Andresen, J.M., 2020. Environ. Geochem. Health 42, 1507–1515.

Gozali Balkanloo, P., Mahmoudian, M., Hosseinzadeh, M.T., 2020. Chem. Eng. J. 396.

Kosicki, R., Błajet-Kosicka, A., Grajewski, J., Twarużek, M., 2016. Animal Feed Sci. Technol 215, 165–180.

Mao, J., Lv, G., Zhou, R., 2020. Environ. Sci. Pollut. Res. Int. 27, 4284–4293.

Mosaleheh, N., Sarvi, M.N., 2020. Environ. Res. 182, 109056.

Nguyen Van, H., Chu Van, H., Luu Hoang, T., Vo Nguyen, D.K., Ha Thuc, C.N., 2020. Arabian J. Chem. 13, 7212–7223.

Pavlidou, S., Papaspyrides, C.D., 2008. Prog. Polym. Sci. 33, 1119–1198.

Phillips, T.D., Afriyie-Gyawu, E., Williams, J., Huebner, H., Ankrah, N.A., Ofori-Adjei, D., Jolly, P., Johnson, N., Taylor, J., Marroquin-Cardona, A., Xu, L., Tang, L., Wang, J.S., 2008. Food Addit. Contam. Part A Chem. Anal. Control Expo Risk Assess 25, 134–145.

Wang, G., Miao, Y., Sun, Z., Zheng, S., 2018. J. Colloid Interface Sci. 511, 67–76.

Wang, G., Xi, Y., Lian, C., Sun, Z., Zheng, S., 2019. J. Hazard. Mater. 364, 227–237.

Zhang, Z.Z., 1993. Environ. Sci. Technol. 27, 6.